Metal−Ligand Delocalization in Magnetic Orbitals of Binuclear Complexes

Jesús Cabrero,[†] Carmen J. Calzado,[‡] Daniel Maynau,[‡] Rosa Caballol,*[,†] and Jean Paul Malrieu[‡]

Departament de Química Física i Inorgànica and Institut d'Estudis Avançats, Universitat Rovira i Virgili, Pl. Imperial Tarraco 1, 43005 Tarragona, Spain, and Laboratoire de Physique Quantique, IRSAMC, Université Paul Sabatier, 118 route de Narbonne, 31062 Toulouse, France

Received: February 15, 2002; In Final Form: June 14, 2002

The nature of magnetic orbitals is analyzed on a series of five $Cu(d^9)\cdots Cu(d^9)$ complexes, comparing various theoretical approaches. The magnetic orbitals are usually defined from ab initio mean-field calculations. It is shown that they are practically identical for the lower and upper multiplets. Diagonalization of the density matrices obtained from accurate configuration interaction wave functions provides natural magnetic orbitals, which should be considered as the reference information. No appreciable differences between the natural orbitals of both states are observed. The natural magnetic orbitals are significantly more delocalized on the ligands than the mean-field ones. It is shown that the definition of magnetic orbitals from spin-unrestricted density functional theory (DFT) calculations is not straightforward. When carefully determined, the DFT magnetic orbitals appear to strongly overestimate the metal−ligand delocalization. The consequences on the spin density are discussed.

1. Introduction

Understanding the magnetic properties of polyradicalar systems in which several (at least two) sites bear unpaired electrons is a crucial step for the chemists involved in the design of magnetic materials.[1−3] The interaction between the magnetic centers can be described with an effective spin-only Hamiltonian as the Heisenberg−Dirac−Van Vleck Hamiltonian:[4]

$$\hat{H} = -\sum_{i,j} J_{ij} \vec{S}_i \vec{S}_j \tag{1}$$

where J_{ij} is the magnetic coupling between the electrons in sites i and j. For two particles, the Heisenberg Hamiltonian is

$$\hat{H} = -J \vec{S}_1 \vec{S}_2 \tag{2}$$

and it is easy to show that for centers with $M_s = \pm 1/2$ the magnetic coupling is just the difference between the energies of the singlet and the triplet states, $J = {}^1E - {}^3E$, J being positive when the system is ferromagnetic (the triplet state is the ground state) and negative when it is antiferromagnetic (the ground state is the singlet one). The sign and magnitude of J depend on the extension and the nature of the interactions between the magnetic centers. In the qualitative pictures, two opposite contributions are distinguished: the ferromagnetic contribution (F), coming from the direct exchange between the magnetic centers, $2K$, which is always a positive value, and an antiferromagnetic (thus negative) contribution, due to the delocalization effects. This antiferromagnetic (AF) contribution can be expressed as $-4t^2/U$, where t is the electron-transfer integral between the magnetic orbitals and U is the repulsive interaction of two electrons placed in the same magnetic orbital(*on-site* repulsion):[5]

$$J = J_F + J_{AF} = 2K - \frac{4t^2}{U} \tag{3}$$

Several simple models have been proposed to understand the balance between the direct exchange, favoring ferromagnetism, and intersite electronic delocalization, acting in favor of antiferromagnetism. Such models may be formulated in terms of nonorthogonal valence bond (VB) concepts,[6,7] valence configuration interaction,[8] or orthogonal valence bond.[5,8,9] These qualitative interpretations face two problems. The first one concerns the definition of the magnetic orbitals themselves.[10] This question is addressed in the present paper, which also discusses the content of the density functional theory (DFT) calculations in terms of effective interactions between magnetic orbitals. The second problem arises from the quantitative failure of the valence-only description to reproduce the J coupling when handling the exact Hamiltonian.[11−16] An analysis of the respective role of the intravalence and the external correlation effects (spin polarization, dynamic polarization of the ionic VB structures, etc.) has been given recently.[17]

The term "magnetic orbitals", commonly used in all of these approaches, refers to localized orbitals centered on the magnetic sites with appropriate tails on the surrounding and bridging ligands. Their definition is somewhat ambiguous and deserves to be discussed. The present paper analyzes three definitions of orthogonal magnetic orbitals. The simplest one relies on the mean-field Hartree−Fock (HF) description of, for instance, the upper multiplet of the complex. Similar definitions may be obtained from DFT calculations of the upper multiplet, now using exchange−correlation parametric potentials instead of the exact Hamiltonian, provided that a correct identification of the singly occupied orbitals is performed. The most rigorous definition of the magnetic orbitals is obtained by considering

[†] Universitat Rovira i Virgili.
[‡] Université Paul Sabatier.

10.1021/jp0204410 CCC: $22.00
Published on Web 08/09/2002

the natural orbitals, that is, the eigenvectors of the exact density matrix. Highly correlated wave functions from large configuration interaction (CI) expansions provide accurate values of the magnetic coupling constants and quite accurate density matrices. The corresponding natural magnetic orbitals may be considered as the most exact ones. In principle, they may be different for the different multiplets, but they are practically indistinguishable in the systems analyzed here. The mean-field magnetic orbitals and the DFT ones are to be compared to these benchmark natural magnetic orbitals. As will be shown, a crucial difference concerns the extent of delocalization between the metal and the ligands, especially the bridging ones.

Four different antiferromagnetic (AF) systems have been considered in the present work, all of them involving two electrons on two Cu(d^9) sites. Three of them are binuclear complexes and the last one is a fragment of a periodic lattice: (i) the $[Cu_2Cl_6]^{2-}$ complex in a planar geometry, leading to a weak AF coupling ($J = -40$ cm^{-1}, 0 cm^{-1});[18] (ii) the $[Cu_2(\mu\text{-}N_3)_2(NH_3)_6]^{2+}$ complex with end-to-end bridging azido-ligands ($J < -800$ cm^{-1});[19] (iii) the $Cu_2(\mu\text{-}CH_3COO)_4(H_2O)_2$ molecule with four acetato-bridges ($J = -286$ cm^{-1}, -294 ± 4 cm^{-1});[20,21] (iv) the Cu_2O_7 cluster embedded in a set of pseudo-potentials and point charges, representing the La_2CuO_4 periodic lattice ($J = -1032 \pm 48$, -1081 ± 40 cm^{-1}).[22,23] A ferromagnetic (F) $[Cu_2Cl_6]^{2-}$ complex has also been considered. Its structure differs from the AF complex one in a twist of the bridge that changes the square-planar coordination of the copper center to a distorted tetrahedral one ($J = +93$ cm^{-1}).[24]

The chemical nature and orientation of the bridging ligands are very different, and this set can be considered as a reasonable sample of binuclear biradical-type systems. The results show very significant trends. They indicate that the dynamical correlation significantly increases the delocalization between the metal and the ligands, the HF magnetic orbitals being too localized. Oppositely, the DFT orbitals are too delocalized.

2. Definition of Orthogonal Magnetic Orbitals

2.1. General Considerations. Let us consider a binuclear complex A$^{\bullet}$— L — B$^{\bullet}$, where A and B are supposed to bear an unpaired electron and L stands for closed-shell ligands. Such terms are typical of a molecular orbital (MO) model with doubly occupied MOs and two unpaired electrons in two singly occupied orthogonal orbitals, *a* and *b*, essentially located on A and B, respectively.

The single-configuration descriptions of the triplet (with $M_s = +1, 0, -1$) and singlet states are

$$T^+_{ab} = |\cdots h\bar{h}\cdots l\bar{l}ab\rangle \qquad T^-_{ab} = |\cdots h\bar{h}\cdots l\bar{l}\bar{a}\bar{b}\rangle$$

$$T^0_{ab} = \left|\frac{1}{\sqrt{2}}\cdots h\bar{h}\cdots l\bar{l}(a\bar{b} - b\bar{a})\right\rangle$$

$$S_{ab} = \left|\frac{1}{\sqrt{2}}\cdots h\bar{h}\cdots l\bar{l}(a\bar{b} + b\bar{a})\right\rangle \quad (4)$$

The $|a\bar{b}\rangle$ and $|b\bar{a}\rangle$ determinants correspond to situations with one electron on each magnetic center (neutral determinants), while $|a\bar{a}\rangle$ and $|b\bar{b}\rangle$ correspond to ionic situations with both active electrons on the same magnetic center.

If A and B are identical, the structure belongs at least to the C_i point group and the two *a* and *b* orbitals generate symmetry-adapted *g* and *u* orbitals:

$$g = \frac{a+b}{\sqrt{2}} \quad \text{and} \quad u = \frac{a-b}{\sqrt{2}} \quad (5)$$

and the three components of the T_u triplet and the purely neutral S_N singlet are

$$T^+_u = |\cdots h\bar{h}\cdots l\bar{l}gu\rangle = T^+_{ab} \qquad T^-_u = |\cdots h\bar{h}\cdots l\bar{l}\bar{g}\bar{u}\rangle = T^-_{ab}$$

$$T^0_u = \left|\frac{1}{\sqrt{2}}\cdots h\bar{h}\cdots l\bar{l}(g\bar{u} - u\bar{g})\right\rangle = T^0_{ab}$$

$$S_N = \left|\frac{1}{\sqrt{2}}\cdots h\bar{h}\cdots l\bar{l}(g\bar{g} - u\bar{u})\right\rangle = S_{ab} \quad (6)$$

The use of nonorthogonal orbitals a' and b',

$$a' = \alpha a + \beta b \quad \text{and} \quad b' = \beta a + \alpha b \quad (7)$$

in a broken-symmetry and spin-contaminated approach of the singlet $|l'\bar{l}'a'\bar{b}'\rangle$ introduces some ionic component in the wave function, but this mixture is meaningless for the triplet state, and it is preferable to remain in an orthonormal set.

The correct magnetic orbitals cannot be pure atomic orbitals, not only because of the orthogonality constraint but also because of an important electronic delocalization between the metal and the ligand. In particular, the ligand orbitals, of lower energy than the metal unpaired ones, take bonding (in phase) tails on the atomic-like 3d orbital of the metal, to give a stabilized *l* orbital, while the *a* orbital has antibonding (out of phase) tails on the ligand[3], as shown in the following scheme:

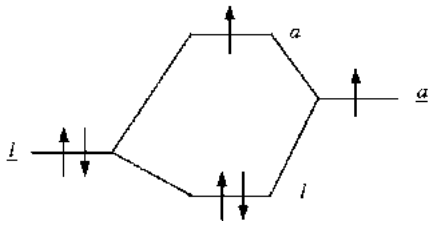

This is a basic feature in these architectures: the in-phase delocalization takes place primarily in the doubly occupied orbitals and, as a consequence of this phenomenon, tails appear in the opposite (out of phase) direction in the singly occupied MOs, the tails depending on the energy difference between $\underline{a}$ and $\underline{l}$. The whole physics of the magnetic coupling is largely dominated by the amplitudes of $\underline{a}$ and $\underline{b}$ on the bridging ligand (or of the ligand $\underline{l}$ orbitals on *a* and *b*), because the bridge is the spatial region where the two unpaired electrons may interact. As will be shown in section 4, the tails are nonnegligible and their amplitude depends strongly on the level of description.

2.2. Mean-Field Determination of the Orbitals. The simplest way to obtain the orbitals is to minimize the single-determinant self-consistent field (SCF) energy of the upper multiplet, here the T^+_u triplet (or any other component T^-_u, T^0_u). To avoid spin contamination and symmetry breaking, the restricted open-shell Hartree−Fock (ROHF) procedure is to be used. This procedure defines an optimal set of symmetry-adapted molecular orbitals, among which the *g* and *u* singly occupied ones may give the *a* and *b* localized magnetic orbitals by the inverse rotation:

$$a = \frac{g+u}{\sqrt{2}} \quad \text{and} \quad b = \frac{g-u}{\sqrt{2}} \quad (8)$$

Most post-Hartree−Fock calculations of both states start from this convenient set. An objection that may be raised is that this choice introduces a bias in favor of the triplet. It is actually possible to obtain a two-configuration SCF descrip-

TABLE 1: Natural Orbital Occupation Numbers for Five Different Systems[a]

NO	AF $[Cu_2Cl_6]^{2-}$	F $[Cu_2Cl_6]^{2-}$	$[Cu_2(\mu\text{-}N_3)_2(NH_3)_6]^{2+}$	$Cu_2(\mu\text{-}CH_3COO)_4(H_2O)_2$	Cu_2O_7
occupied	1.978, 1.972	1.982, 1.983	1.982, 1.990	1.985, 1.990	1.985, 1.980
magnetic	1.088, 0.964	1.016, 1.010	1.142, 0.874	0.956, 1.066	1.142, 0.897
virtual	0.006, 0.006	0.007, 0.006	0.008, 0.006	0.007, 0.006	0.006, 0.004

[a] The numbers concern the less doubly occupied MOs, active MOs, and the most occupied virtual MOs.

tion of the singlet state,

$$S_g = \lambda|\cdots h\bar{h}\cdots l\bar{l}g\bar{g}\rangle - \mu|\cdots h\bar{h}\cdots l\bar{l}u\bar{u}\rangle \qquad \lambda, \mu > 0 \qquad (9)$$

by optimizing both the MOs and the λ/μ ratio in a multiconfiguration self-consistent field (MCSCF) procedure. This wave function introduces an ionic VB component in the purely neutral S_N singlet wave function because it can be written as

$$S_g = (\lambda + \mu)\left|\cdots h\bar{h}\cdots l\bar{l}\left(\frac{a\bar{b} + b\bar{a}}{\sqrt{2}}\right)\right\rangle + (\lambda - \mu)|\cdots h\bar{h}\cdots l\bar{l}\left(\frac{a\bar{a} + b\bar{b}}{\sqrt{2}}\right)\rangle \qquad (10)$$

For the biradicals described here, it happens that the g and u orbitals obtained in the T_u^+ triplet and the S_g singlet SCF calculations are almost identical, as can be concluded by comparing their shapes. More quantitatively, we have calculated the difference of amplitudes between the triplet and the singlet magnetic orbitals. This difference nowhere exceeds 10^{-3} and hereafter only the triplet ROHF MOs are used.

2.3. Natural Orbitals. Many previous works[11−16] have shown that the mean-field level does not give a reasonable estimate of the magnetic coupling constant, J, despite the inclusion of ionic VB structures in the S_g state, eq 10, that reflect the specific electronic delocalization in the singlet state, argued by Anderson[5] to be responsible for the antiferromagnetism. The difference dedicated configuration interaction (DDCI) method[25] has been shown to provide very accurate values of J for a wide range of systems.[14,26−28] It starts from the minimal valence-only complete active space (CAS), including two electrons in two orbitals (g and u or a and b) for the $Cu^{2+}\cdots Cu^{2+}$ systems, and performs a CI including all single and double substitutions on top of it, excluding the double excitations, which involve two inactive occupied and two inactive virtual orbitals. It has been demonstrated[25,29] that these purely inactive double substitutions, at least up to the second order of perturbation theory, lead to a common energy shift on both the singlet and the triplet and consequently do not contribute to the energy gap. Despite avoiding these inactive double substitutions (which are the most numerous ones), the DDCI expansions on organometallic complexes, using nonminimal basis sets, easily exceed 10^6 determinants.

From the wave function of the singlet and of the triplet states, it is possible to build the singlet and triplet one-electron density matrices, $^S\mathbf{R}$ and $^T\mathbf{R}$. The state-specific natural orbitals (NOs) obtained for our models give, as before, differences of the amplitude of the orbitals of both states that nowhere exceed 10^{-3}. Furthermore, as shown previously,[30−33] it is possible to consider the average density matrix $\bar{\mathbf{R}} = (^S\mathbf{R} + {}^T\mathbf{R})/2$. Its diagonalization provides mean natural orbitals:

$$\bar{\mathbf{R}}\bar{\varphi}_i = \bar{n}_i\bar{\varphi}_i \qquad (11)$$

The density matrices $^S\mathbf{R}$ and $^T\mathbf{R}$ should be calculated from wave functions including all possible double excitations, but the size of CASSDCI (all singles and doubles on top of the CAS) calculations in the studied systems exceeds usual technical possibilities, and the highest level available eigenvectors are those resulting from a DDCI calculation. In section 4, a comparison between the NOs from a CASSDCI and those resulting from a DDCI subspace calculation is shown in the simplest AF $[Cu_2Cl_6]^{2-}$ system. The similarity between both sets of NOs is such that hereafter the NOs obtained from the DDCI wave functions are used as the reference ones.

The NO occupation numbers, $\bar{n}_i$, are well contrasted: they are very close to 2 for the orbitals corresponding to the closed shell levels, and close to 0 for the virtual levels, the magnetic NOs being identified as the two eigenvectors with occupation numbers close to 1. To illustrate this assertion, the occupation numbers closest to 1 for the five systems are given in Table 1. The contrast between essentially doubly occupied, magnetic and essentially virtual NOs is manifest and allows easy identification of the magnetic orbitals in a post-Hartree−Fock calculation.

To improve the quality of the description and to make the results independent of the choice of the MOs used in the calculation, the CI step may be repeated. Starting from the first NOs, a new DDCI calculation giving new density matrices and new NOs is performed, and the procedure, called iterative difference dedicated CI (IDDCI),[32] is iterated to convergence.

2.4. DFT Magnetic Orbitals. The study of magnetic systems from DFT methods usually proceeds through Noodleman's approach.[34] The M_s = max (here 1) upper multiplet component is calculated in the unrestricted formalism, which makes the α and β spin orbitals slightly different and produces some spin contamination. The corresponding wave function is

$$T^+_{UHF} = |\cdots h_\alpha\overline{h}_\beta\cdots l_\alpha\overline{l}_\beta\cdots ab\rangle = |\cdots h_\alpha\overline{h}_\beta\cdots l_\alpha\overline{l}_\beta\cdots g_\alpha u_\alpha\rangle \qquad (12)$$

The identification of the singly occupied molecular orbitals (SOMOs) in T^+_{UHF} is not straightforward, as reported in previous studies,[35,36] because this wave function is invariant under rotation of the occupied α (respectively β) spin orbitals. Several options are possible to obtain the SOMOs. Unrestricted natural orbitals (UNO) may be calculated by using the proper keyword in the Gaussian 98 package.[37] Projection techniques (PO) have also been described.[38] Although both procedures are not equivalent, it has been verified that in the systems presented here the two sets of orbitals, UNO and PO, hereafter called α-SOMOs, are practically indistinguishable.

The energy of the singlet state is approached through the calculation of a broken symmetry $M_s = 0$ solution:

$$S^{BS} = |\cdots h_\alpha^{BS}\overline{h}_\beta^{BS}\cdots l_\alpha^{BS}\overline{l}_\beta^{BS}\cdots a^{BS}\overline{b}^{BS}\rangle \qquad (13)$$

The $\hat{S}^2$ mean value of this function is usually very far from that of a singlet, close to an equal mixture of a singlet and a triplet. Noodleman's expression for the singlet−triplet gap is[39−41]

$$\Delta E_{ST} = \frac{2(E_{S^{BS}} - E_{T^+_{UHF}})}{1 + S^2_{ab}} \qquad (14)$$

where S_{ab} is the overlap between a^{BS} and b^{BS}. Because the distance between the magnetic centers is usually large, S_{ab}^2 is small (when calculated in the complexes discussed here, S_{ab}^2

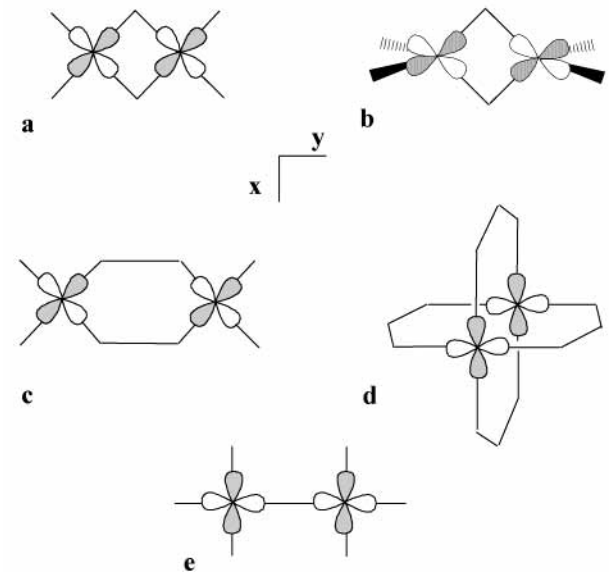

Figure 1. Schematic representation of the five considered models: (a) the AF $[Cu_2Cl_6]^{2-}$ complex, in a planar geometry; (b) the F $[Cu_2Cl_6]^{2-}$ complex, in a distorted geometry; (c) the $[Cu_2(\mu\text{-}N_3)_2(NH_3)_6]^{2+}$ complex, with end-to-end bridging azido ligands; (d) the $Cu_2(\mu\text{-}CH_3COO)_4(H_2O)_2$ molecule; (e) the Cu_2O_7 cluster, a fragment of the La_2CuO_4 lattice.

never exceeds 0.1, see ref 42) and in general the S−T gap may be approximated by[39,40]

$$\Delta E_{ST} = 2(E_{SBS} - E_{T^+_{UHF}}) \qquad (15)$$

The denominator in expression 14 is much closer to 1, and therefore, it is artificial to divide expression 15 by 2.

In the broken-symmetry solution, a^{BS} and b^{BS} are nonorthogonal; their tails on the neighbor site introduce an ionic component in the wave function, cf. eq 7. To compare DFT and ab initio orbitals, the triplet DFT state is to be used to keep the orthogonality.

3. Computational Details

The five systems considered here (Figure 1) contain two Cu(d^9) centers, bridged by different ligands and with different relative positions. The first model is the $[Cu_2Cl_6]^{2-}$ complex, of which the magnetostructural dependence has been extensively studied in the recent past.[43] Two different geometries have been considered, namely, the planar structure (Figure 1a), giving AF coupling, and the distorted (Figure 1b) structure, in which the external ligands plane is twisted ($\tau = 45°$) with respect to the bridge plane, giving F coupling. The three remaining AF systems are the $[Cu_2(\mu\text{-}N_3)_2(NH_3)_6]^{2+}$ complex (Figure 1c), the $Cu_2(\mu\text{-}CH_3COO)_4(H_2O)_2$ molecule (Figure 1d), and a model of the antiferromagnetic perovskite La_2CuO_4, the Cu_2O_7 cluster (Figure 1e), embedded in a set of point charges to mimic the Madelung field of the La_2CuO_4 lattice. A more extended description of the four antiferromagnetic compounds, as well as the computational details regarding the basis sets and the effective core potentials (ECP) used in ab initio CI calculations, can be found in ref 17. Regarding the DFT calculations, the B3LYP parametrization has been used. The basis sets and ECP used for the AF systems can be found in ref 42. The basis sets used for the ferromagnetic $[Cu_2Cl_6]^{-2}$ complex are the same as for the AF one.

The ROHF molecular orbitals have been obtained by using the MOLCAS 4.1 package.[44] The CASDI[45] and the NATURAL[46] programs have been used in the CI calculations and in the determination of the natural MOs. All DFT calculations have been performed by means of the Gaussian 98 code.[37] MOLDEN code[47] has been used to represent the MOs.

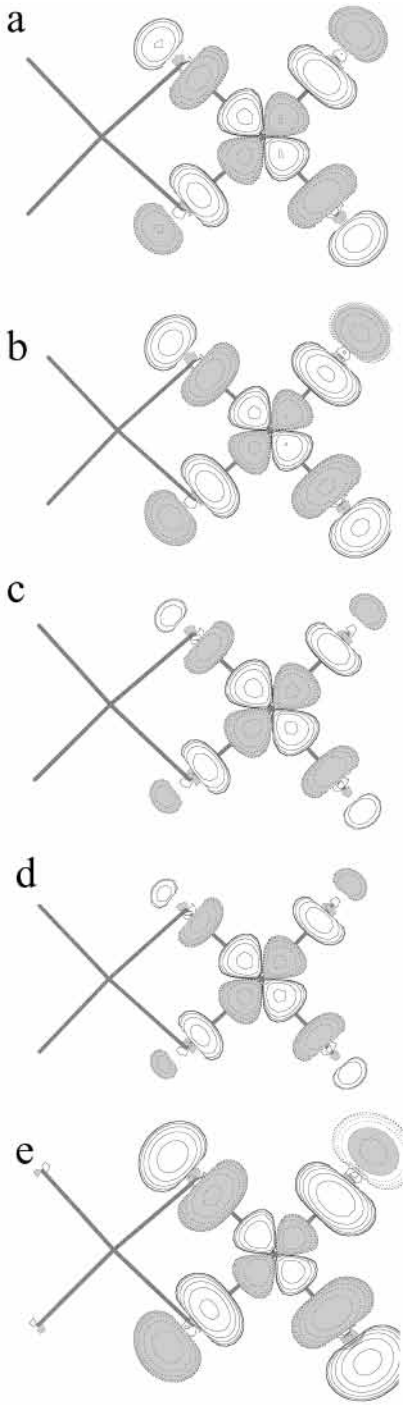

Figure 2. Shapes of the $a = (g + u)/\sqrt{2}$ localized orbital for the AF $[Cu_2Cl_6]^{2-}$ complex obtained with different approaches: (a) CASSDCI NOs; (b) DDCI NOs; (c) DDCI2 NOs; (d) ROHF MOs; (e) B3LYP α-SOMOs.

4. Results and Discussion

4.1. Extent of the Metal−Ligand Delocalization. Let us discuss first in detail the results for the AF planar $[Cu_2Cl_6]^{2-}$ complex. Figure 2 presents the shapes of the localized magnetic orbitals obtained at different levels of calculation. As expected, all sets present the same out-of-phase delocalization tails between the copper d orbital and the neighboring ligands (the

TABLE 2: Cu 3d Mulliken Population Corresponding to the Magnetic Orbitals from Different Theoretical Approaches and the Spin Density on Cu Atoms in the F $[Cu_2Cl_6]^{-2}$ Complex (in parentheses)

	DDCI		B3LYP		
	NOs	ROHF	α-highest	β-LUMO	α-SOMO
AF $[Cu_2Cl_6]^{2-}$	0.72	0.91	0.10	0.47	0.48
$[Cu_2(\mu\text{-}N_3)_2(NH_3)_6]^{2+}$	0.80	0.94	0.23	0.61	0.63
$Cu_2(\mu\text{-}CH_3COO)_4(H_2O)_2$	0.88	0.94	0.16	0.71	0.73
Cu_2O_7	0.75	0.90	0.31	0.68	0.69
F $[Cu_2Cl_6]^{-2}$	0.73	0.92			0.51
	(0.71)	(0.94)			(0.46)

bonding combination belonging to the doubly occupied subset), but the extent of the metal−ligand mixing is strongly dependent on the method.

The NOs resulting from the CASSDCI calculations, including the self-consistent size-consistent (SC^2) correction[48] for open-shell systems[49] can be considered as the most exact accessible ones. These magnetic NOs (Figure 2a) present a significant metal−ligand delocalization. The DDCI NOs (Figure 2b) are practically identical to the precedent ones. This justifies that for the remaining systems DDCI NOs are considered as the reference ones. The difference dedicated configuration interaction technique introduces all of the low-order contributions of the dynamical electronic correlation to the energy differences, in particular, to the exchange magnetic coupling as shown recently.[17] As shown in Table 3, the method provides accurate values for the singlet−triplet splitting. The J values obtained with the DDCI approach appear to be much closer to the experimental values than those resulting from DFT calculations.

Figure 2c presents NOs obtained at the DDCI2 level. This CI level omits the double excitations involving two inactive occupied MOs and one inactive virtual MO (referred to as 2h-1p) and those involving one inactive occupied MO and two inactive virtual MOs (1h-2p).[43d] This CI level is introduced here to discuss the role of the dynamical correlation, as discussed in section 4.2. The corresponding NOs appear to be less delocalized than CASSDCI and DDCI ones.

Figure 2d represents the ROHF localized orbitals, which are much more concentrated on the metal than the magnetic natural MOs obtained at the CASSDCI and DDCI levels. Figure 2e plots the localized singly occupied magnetic orbitals, α-SOMOs, of the unrestricted triplet-state B3LYP calculations. The amplitudes on the ligands are much larger than those in the ROHF calculations and even than those in the best CI ones.

As a minor methodological point, the risks of using incorrect definitions of the magnetic orbitals in unrestricted methods are illustrated in Figure 3. Localized B3LYP α-MOs obtained from the highest g and u symmetry-occupied α subset of the unrestricted triplet state are shown in Figure 3a. They exhibit physically meaningless delocalization tails, spanning up to the nonadjacent ligands. In contrast, the β lowest unoccupied MOs (Figure 3b) provide a description very close to the α-SOMOs. This similarity is related with the weak spin contamination found in the B3LYP triplet of the systems discussed here.

The DDCI, ROHF, and DFT localized magnetic orbitals of the remaining systems are shown in Figures 4−7. The same trend as that for the AF $[Cu_2Cl_6]^{2-}$ is observed when comparing the three types of magnetic orbitals: (i) ROHF underestimates the ligand−metal delocalization and (ii) DFT overestimates this delocalization with respect to DDCI NOs.

To introduce a quantitative measure of the delocalization, Mulliken population analysis has been performed. Table 2 shows the 3d Cu population in the different magnetic orbitals, for the five systems considered. In agreement with the amplitudes of the orbitals, the Cu population decreases from ROHF to B3LYP orbitals. In this last case, the metal-to-ligand delocalization is overestimated, and the extremely low Cu population in the highest occupied α orbitals confirms the observation that these orbitals cannot be considered as the magnetic ones. The Cu population in α-SOMOs is practically identical to that in β-LUMOs, accordingly to the previous comment, but always smaller than that in the natural orbitals. These results show that the metal-to-ligand delocalization (MLD) follows the hierarchy $MLD_{ROHF} < MLD_{NATURAL} < MLD_{DFT}$.

4.2. Role of the Dynamical Correlation. The natural orbitals represent the best one-electron information available from the N-electron-correlated description. Moreover, as shown on the test performed on the AF $[Cu_2Cl_6]^{-2}$ complex, the natural magnetic orbitals coming from the DDCI calculations are practically identical to those obtained from calculations involving all double excitations on top of the same CAS. The natural orbitals obtained from these long CI expansions of the wave functions can be considered with a great reliability as being very close to the exact ones.

The inclusion of dynamical correlation has an important impact on the metal−ligand delocalization on the magnetic orbitals. The natural orbitals have much larger tails on the first-neighbor ligands than the mean-field singly occupied orbitals. It is interesting to analyze which of the different types of double excitations are responsible for the observed increase of metal−ligand delocalization. Figure 2c presents NOs obtained for the AF $[Cu_2Cl_6]^{2-}$ complex at the DDCI2 level, which omits the 2h-1p and the 1h-2p double excitations, as described in section 4.1. These orbitals are significantly less delocalized than those obtained from CASSDCI (Figure 2a) or from the full DDCI expansion (Figure 2b). An analytical demonstration given previously[17] has shown that this additional metal−ligand delocalization is due in particular to the dynamical correlation effects of the two hole−one particle (2h-1p) excitations. This demonstration is numerically confirmed here. In an intuitive picture, or in the so-called "two-band" model, one may say that these double excitations bring the dynamical polarization of the ligand-to-metal charge transfer states or that they decrease the effective energy of these states involved in the spin exchanges between two metallic centers.

4.3. Effect of the Exchange−Correlation Functional in DFT Calculations. The second observation concerns the DFT orbitals. The properly defined α-SOMOs appear to systematically exaggerate the delocalization tails between the metal and the ligands.

The origin of this excess is attributable to the exchange potential as shown by the results in Table 4. This table reports the magnetic coupling constants obtained for the La_2CuO_4 system when a modified B3LYP hybrid functional is used. The original B3LYP exchange−correlation functional[50] can be written as

$$pE_x^{HF} + qE_x^{Slater} + 0.72\Delta E_x^{Becke} + 1.0E_c^{VWN} + 0.81\Delta E_c^{LYP} \quad (16)$$

with $p = 0.2$ and $q = 0.8$, where E_x^{HF} is the Fock exchange, E_x^{Slater} the local Slater exchange,[51] and ΔE_x^{Becke} the nonlocal Becke exchange correction.[52] E_c^{VWN} is the local Vosko, Wilk, and Nusair correlation functional,[53] and ΔE_c^{LYP} is the Lee, Yang, and Parr nonlocal correlation correction.[54] Table 4 shows the values of J obtained when different p and q weights are used. Increasing the Fock exchange contribution decreases the absolute value of the magnetic coupling constant, between the two limits represented by B3LYP and UHF calculations, the

TABLE 3: Magnetic Coupling Constant (in cm^{-1}) Obtained for the Five Systems by Using Different Theoretical Approaches and MO Sets

	AF $[Cu_2Cl_6]^{2-}$	F $[Cu_2Cl_6]^{2-}$	$[Cu_2(\mu\text{-}N_3)_2(NH_3)_6]^{2+}$	$Cu_2(\mu\text{-}CH_3COO)_4(H_2O)_2$	Cu_2O_7
CASCI[a]	+78	+119	−253	−33	−451
DDCI[a]	−15	+96	−1125	−238	−1129
B3LYP	−99	+152	−2779	−557	−1686
expt	−40[18b], 0[18c]	+93[24]	<−800[19]	−286[20]	−1032 ± 48[22]
				−294 ± 4[21]	−1081 ± 40[23]

[a] In the CI calculations, iterated NOs have been used.

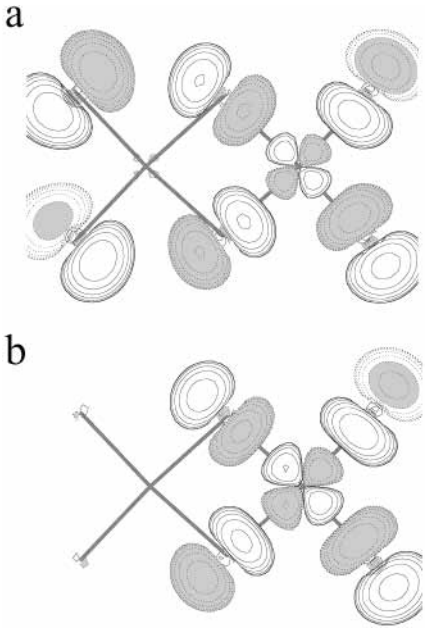

Figure 3. Shapes of the *a* localized orbital for the AF $[Cu_2Cl_6]^{2-}$ complex at the B3LYP level obtained from (a) the highest α occupied MOs and (b) the lowest β unoccupied MOs.

overestimation being even larger when no hybrid functional is used.[55] This is a general behavior also found in the evaluation of other observables (the hopping integral in mixed-valence systems,[56] the strength of the three-electron hemibonded structures of $(H_2O)_2^+$ (ref 57), etc.).

Figure 8 shows the shapes of the localized α-SOMO for the La_2CuO_4 system for three-limit cases: on the top, the localized magnetic orbital coming from the unrestricted Hartree−Fock triplet state; in the middle, the same orbital but obtained by mixing 1:1 Fock and Slater exchange functionals ($p = q = 0.5$ in eq 16); at the bottom, the B3LYP localized magnetic orbital. Decreasing the Fock contribution increases the delocalization toward the oxygen ligands, that is, the magnetic orbitals show a smaller concentration on the metal. It is worth noticing that, as reported before,[55] the correlation potential has no effect on the magnetic coupling (in Table 4, UHF value versus $p = 1.0$), indicating that the increase of J in DFT versus UHF is solely an effect of the exchange potential. Finally, the comparison between Figures 7b and 8a and the Mulliken populations in Tables 2 and 4 indicates that the restricted and the unrestricted triplet calculations give an equivalent metal−ligand delocalization.

The relationship between the J value and the magnetic orbitals is clearly illustrated in Figure 9, corresponding to the La_2CuO_4 system. On the bottom, the Cu 3d Mulliken population in the magnetic orbitals is reported versus the percentage of Fock exchange. As mentioned above, the highest α orbitals obtained from a B3LYP calculation ($p = 0.2$ in Figure 9) are excessively delocalized on the ligands (3d population lower than 0.3*e* for all the p values considered). As a minor point, it may be

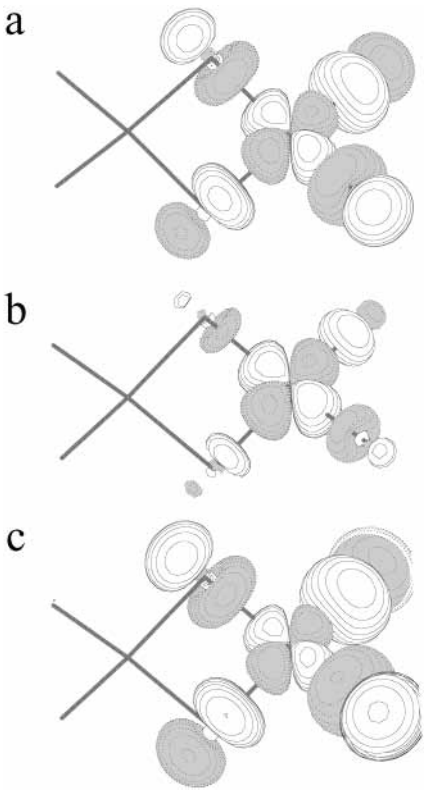

Figure 4. Shapes of the localized *a* orbital for the F $[Cu_2Cl_6]^{-2}$ complex obtained with different approaches: (a) DDCI NOs; (b) ROHF MOs; (c) B3LYP α-SOMOs.

observed that up to 50% of exchange mixing, that is, $p = 0.5$, the β-LUMOs can be considered as the magnetic ones and they turn out to be identical to the projected α-SOMOs, while the use of the projection procedure is necessary for larger percentages.

In a previous paper,[42] we have established that for the La_2CuO_4 system a $p \cong 0.33$ mixing of the exchange potential provides the following: (i) a correct value of J (-1129 cm^{-1}); (ii) a reasonable value of the hopping integral, t_{ab}, and the on-site effective repulsion, U ($t_{ab}^{DFT} = -0.48$ eV, $U^{DFT} = 6.4$ eV) in good agreement with the best values obtained from the most elaborated CI calculations through the effective Hamiltonian theory[42] ($t_{ab}^{eff} = -0.507$ eV, $U^{eff} = 7.3$ eV).

Figure 9 shows that the same percentage of Fock exchange in DFT also gives the correct magnetic orbital Mulliken population in the Cu 3d orbitals, that is, the correct metal−ligand delocalization. This general agreement is consistent because the extent of the magnetic orbitals on the bridging ligands governs both the hopping integral amplitude and the on-site repulsion: as the extension becomes larger, the hopping integral in absolute value becomes larger and the on-site Coulombic repulsion becomes smaller.

We have also performed the same type of calculations for the remaining systems. The results for all of them give similar

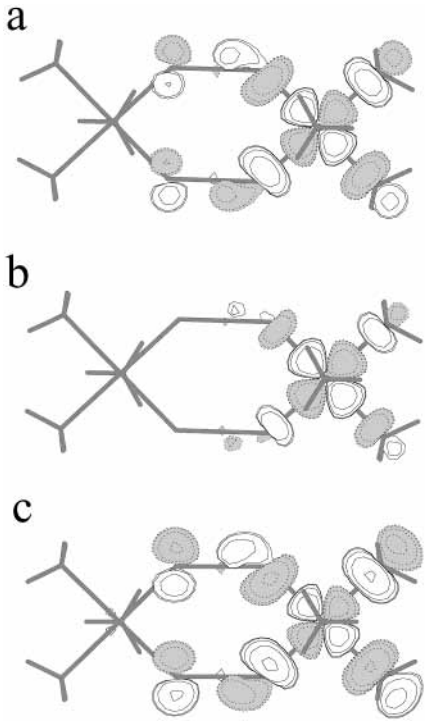

Figure 5. Shapes of the localized *a* orbital for the $[Cu_2(\mu\text{-}N_3)_2(NH_3)_6]^{2+}$ complex obtained with different approaches: (a) DDCI NOs; (b) ROHF MOs; (c) B3LYP α-SOMOs.

conclusions for the percent of Fock exchange reproducing the DDCI NO coupling constant (see Table 3) with the following ratios: 42% for AF $[Cu_2Cl_6]^{2-}$, 50% for F $[Cu_2Cl_6]^{2-}$, 45% for $[Cu_2(\mu\text{-}N_3)_2(NH_3)_6]^{2+}$, and 39% for $Cu_2(\mu\text{-}CH_3COO)_4(H_2O)_2$. It is necessary to slightly increase these ratios (by 2−5%) to reproduce the ab initio Mulliken populations, with the exception of $Cu_2(\mu\text{-}CH_3COO)_4(H_2O)_2$, which needs around 55% Fock exchange to reproduce them. It may be concluded that the balance giving the DDCI reference *J* are similar but not exactly the same for all compounds and that Mulliken populations follow the same trend although there is not a strict correspondence.

4.4. Spin Density. The extent of the delocalization of the magnetic orbitals on the ligands is not only crucial for the *J* values but is related to the spin density distributions, as evident from the single-determinant description of the triplet state. It is expected that a larger delocalization of the magnetic MOs on the ligand is associated with a smaller spin density on the Cu atoms. The spin densities on Cu at various levels of description are reported in Table 2 for the F $[Cu_2Cl_6]^{-2}$ complex. According to the importance of the ligand−metal delocalization, the ROHF spin density on Cu appears to be overestimated, while the B3LYP one appears to be underestimated with respect to the DDCI estimates. The excess of delocalization is also effective in the $M_s = 0$ broken-symmetry B3LYP solution, which takes an exaggerate ionic VB component (i.e., closed-shell character) leading to the well-known overestimation of *J*[39,40,55] (provided that the correct Noodleman's expression (eqs 14 and 15) is used). This argument is in agreement with the fact that in the antiferromagnetic coupling between the high-spin center Mn(II) and the low-spin center Cu(II) in Mn(II)−Cu(II) binuclear compounds, the B3LYP spin densities are found to be significantly smaller than those obtained from polarized neutron diffraction experiments.[58] The same trend has been found in the end-on azido doubly bridged Cu(II) binuclear complexes, in which the atomic spin densities calculated with B3LYP[59] and Becke−Perdew functionals[60] are underestimated with respect to those determined from polarized neutron diffraction studies.[60] In contrast, a correct spin density is obtained for this compound when using DDCI methods.[61]

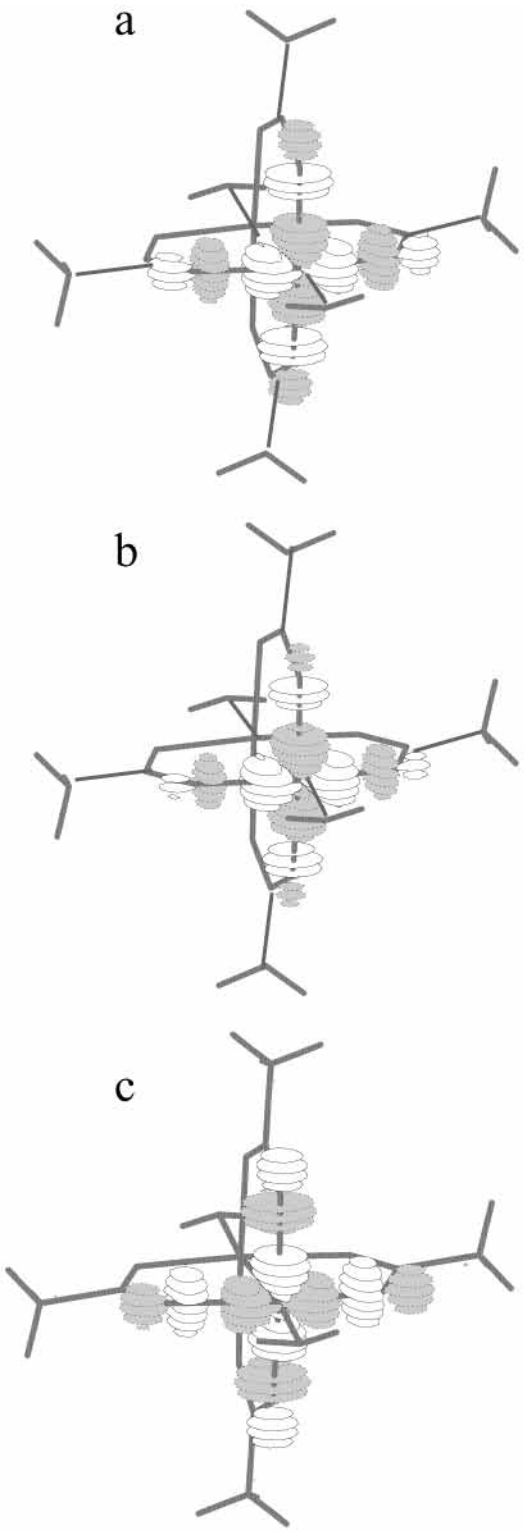

Figure 6. Shapes of the localized *a* orbital for $Cu_2(\mu\text{-}CH_3COO)_4(H_2O)_2$ obtained with different approaches: (a) DDCI NOs; (b) ROHF MOs; (c) B3LYP α-SOMOs.

5. Conclusion

Qualitative models that try to interpret the sign and magnitude of the magnetic coupling constant, *J*, between the unpaired

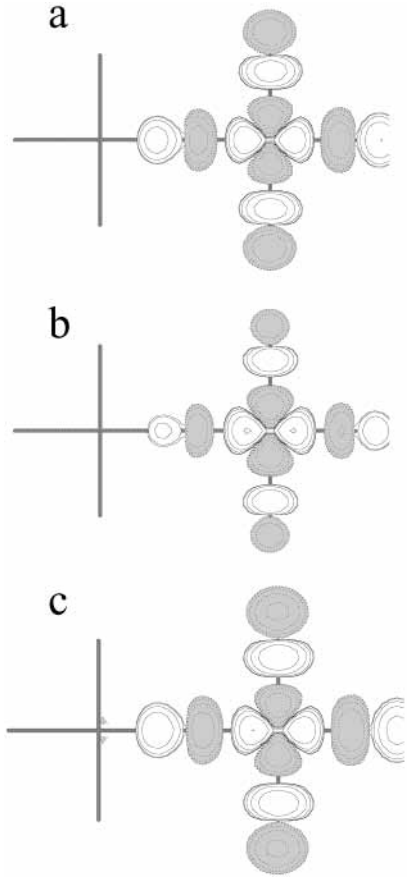

Figure 7. Shapes of the localized *a* orbital for the La_2CuO_4 lattice fragment, obtained with different approaches: (a) DDCI NOs; (b) ROHF MOs; (c) B3LYP α-SOMOs.

TABLE 4: Magnetic Coupling Constant (in cm^{-1}) and Cu 3d Mulliken Population in the Magnetic Orbitals Obtained for the La_2CuO_4 System Versus the Fock (*p*) and Slater (*q*) Exchange Potential Percentage in Hybrid Functionals with the CASCI and DDCI Values Obtained from Natural Orbitals for Comparison

method	*p*	*q*	*J*	Cu 3d
DFT	0.2[a]	0.8[a]	−1686	0.69
	0.3	0.7	−1202	0.74
	0.4	0.6	−895	0.79
	0.5	0.5	−677	0.82
	0.6	0.4	−524	0.85
	1.0	0.0	−282	0.91
UHF			−266	0.92
CASCI			−250	0.75[b]
DDCI			−1129	0.75
expt			-1032 ± 48[22]	
			-1081 ± 40[23]	

[a] B3LYP. [b] With DDCI NOs.

electrons on two distant sites in binuclear complexes are essentially developed in terms of a very restricted space, involving only the unpaired electrons and the so-called "magnetic orbitals". These models rest on intuitive pictures of the magnetic orbitals.[5,7−10] The present paper considers more quantitative definitions of the magnetic orbitals from ab initio and DFT calculations. Mean-field Hartree−Fock orbitals, natural orbitals from high CI levels, and DFT orbitals are compared.

Five $Cu(d^9)\cdots Cu(d^9)$ binuclear complexes involving quite different ligands and orders of magnitude of *J* have been studied. The first conclusion of the work is that the magnetic orbitals for the singlet and triplet states are practically identical at the CASSCF level. This similarity is also observed between the natural orbitals for both states when obtained from extensive CI calculations.

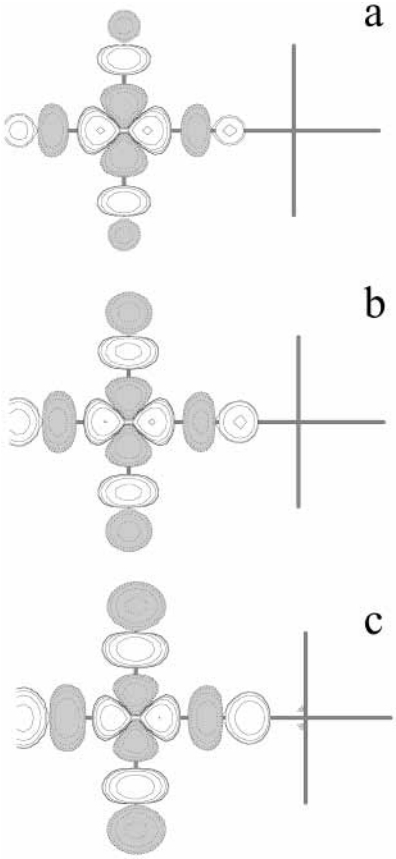

Figure 8. Effect of the mixing of Fock and Slater exchange on the shape of the localized *a* α-SOMO orbital in the Cu_2O_7 cluster: (a) UHF; (b) 50% mixing; (c) B3LYP.

In all approaches, the delocalization between the metal and the ligands is important for the physics of the system. The magnitude of *J* is crucially dependent on its extension. However, the extent of the metal−ligand delocalization, as manifested from the tails of the magnetic orbitals on the ligands (and especially the bridging ligands), are very different from one approach to another. The natural orbitals obtained from DDCI calculations (which accurately reproduce the experimental values of *J*) are close to the most accurate ones, as confirmed by the CASSDCI calculations on the AF $[Cu_2Cl_6]^{-2}$ complex, and can be used as the reference ones. It appears that the following conclusions can be drawn: (i) The mean-field magnetic orbitals are somewhat too localized on the metal atoms. (ii) The dynamical correlation is responsible for the additional metal−ligand delocalization through the specific (2h-1p) double excitations identified in ref 17. (iii) The DFT orbitals, even when properly defined, are excessively delocalized on the ligands. This excess of delocalization, certainly responsible for an overestimation of *J* in the broken-symmetry DFT approaches, is entirely due to the exchange potential. With modification of the ratio of the Fock and the Slater exchange operators, it turns out that a good agreement of the calculated with the experimental value of the coupling constant can be found. At the same time, the corresponding magnetic orbitals are very similar to the magnetic NOs, reflecting a correct amplitude of the delocalization between the metal and the ligands, which is required to obtain correct spin densities on the metal atoms. An optimal ratio between 33% and 50% of Fock exchange is found in the different systems. It indicates that although the trend is preserved, there is no a universal recipe to reproduce

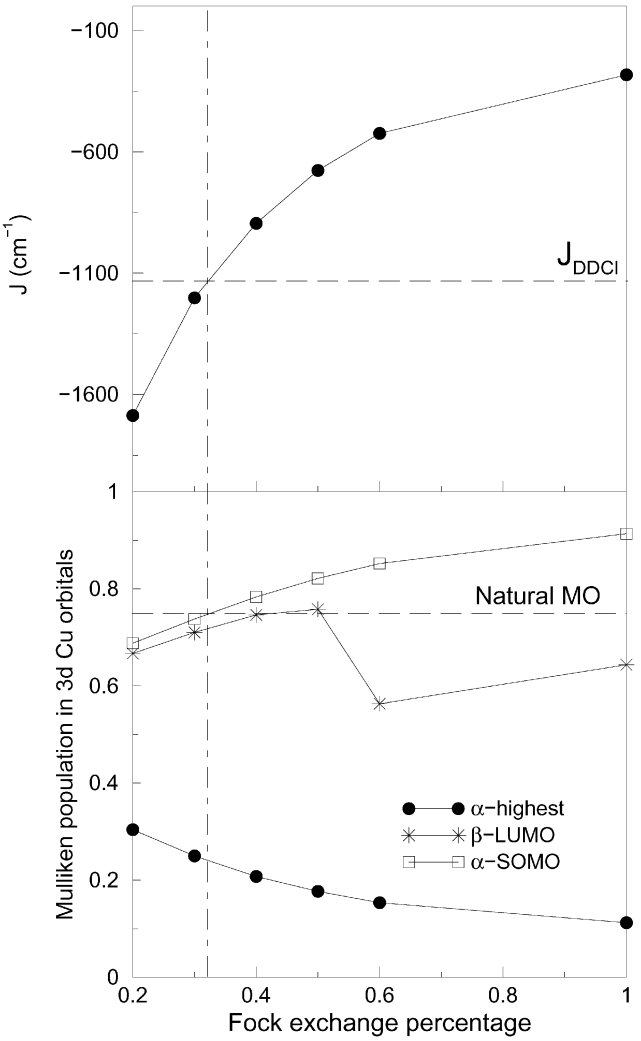

Figure 9. Effect of the increase of Fock exchange on the 3d Cu Mulliken population and J value in the La_2CuO_4 system. On the top, the J value is plotted in cm^{-1}; the vertical dashed line indicates the percentage giving the experimental value. On the bottom, the 3d Cu population for the α-highest occupied orbitals, the β-LUMOs and the projected α-SOMOs is plotted.

all observables in these systems. (iv) The spin density distribution is strongly related to the metal−ligand delocalization, and therefore, the spin density on the metal is overestimated in the ROHF description, while it is underestimated in the B3LYP calculation.

Acknowledgment. The authors are grateful to C. De Graaf for helpful comments and acknowledge the Spanish-French scientific cooperation (Integrated Action HF2000-0030 and PICS2001-13). J.C. and R.C. thank the Spanish Ministery of Science and Technology (Project PB98-1216-CO2-02) and the DURSI of the Generalitat de Catalunya (Grant SGR01-00315) for their financial support. C.J.C. acknowledges the financial support through the TMR activity "Marie Curie research training grants" Grant No. HPMF-CT-1999-00285 of the European Commission. The Laboratoire de Physique Quantique is Unité Mixte (UMR 5626) du CNRS.

References and Notes

(1) Verdaguer, M.; Bleuzen, A.; Marvaud, V.; Vaissermann, J.; Seuleiman, M.; Desplanches, C.; Scuiller, A.; Train, C.; Garde, R.; Gelly, G.; Lomenech, C.; Rosenman, I.; Veillet, P.; Cartier, C.; Villain, F. *Coord. Chem. Rev.* **1999**, *190*−*192*, 1023.

(2) Coronado, E., Delhaès, P., Gatteschi, D., Miller, J. S., Eds. *Molecular magnetism: From molecular assemblies to the devices*; NATO ASI Series E, Applied Sciences, vol. 321; Kluwer: Dordrecht, Netherlands, 1995.

(3) Kahn, O. *Molecular magnetism*; VCH: New York, 1993.

(4) (a) Heisenberg, W. *Z. Phys.* **1928,** *49*, 619. Dirac, P. A. M. *Proc. R. Soc. London A* **1929**, *123*, 714. (b) Dirac, P. A. M. *The principles of quantum mechanics*; Clarendon Press: Oxford, U.K., 1947. (c) Van Vleck, J. H. *The theory of electric and magnetic susceptibilities*; Oxford University Press: Oxford, U.K., 1932.

(5) (a) Anderson, P. W. *Phys. Rev.* **1950**, *79*, 350. (b) Anderson, P. W. In *Theory of the Magnetic Interaction: exchange in insulators and superconductors*; Seitz, F., Turnbul, D., Eds.; Solid State Physics, Vol. 14; Academic Press: New York, 1963; pp 99−124.

(6) Kramers, H. A. *Physica (Amsterdam)* **1934**, *1*, 132.

(7) Kahn, O.; Briat, B. *J. Chem. Soc., Faraday Trans. 2* **1976**, *72*, 268.

(8) Hay, P. J.; Thibeault, J. C.; Hoffmann, R. *J. Am. Chem Soc.* **1975**, *97*, 4884.

(9) (a) Goodenough, J. B. *J. Phys. Chem. Solids* **1958**, *6*, 287. (b) Kanamori, J. *J. Phys. Chem. Solids* **1959**, *10*, 87.

(10) Mouesca, J. M. *J. Chem. Phys*. **2000**, *113*, 10505.

(11) de Graaf, C.; Broer, R.; Nieuwpoort, W. C. *Chem. Phys. Lett*. **1997**, *271*, 372.

(12) Mödl, M.; Dolg, M.; Fulde, P.; Stoll, H. *J. Chem. Phys.* **1997**, *106*, 1836.

(13) Suaud, N.; Lepetit, M. B. *Phys. Rev. B* **2000**, *62*, 402.

(14) (a) Moreira, I. de P. R.; Illas, F. *Phys. Rev. B* **1997**, *55*, 4129. (b) Muñoz, D.; Illas, F.; Moreira, I. de P. R. *Phys. Rev. Lett.* **2000**, *84*, 1579. (c) de Graaf, C.; Moreira, I. de P. R.; Illas, F.; Martin, R. L. *Phys. Rev. B* **1999**, *60*, 3457.

(15) (a) van Oosten, A. B.; Broer, R.; Nieuwpoort, W. C. *Chem. Phys. Lett*. **1996**, *257*, 207. (b) van Oosten, A. B.; Broer, R.; Nieuwpoort, W. C. *Int. J. Quantum Chem., Quantum Chem. Symp.* **1995**, *29*, 241.

(16) Wang, C.; Fink, K.; Staemmler, V. *Chem. Phys. Lett*. **1995**, *102*, 25.

(17) Calzado, C. J.; Cabrero, J.; Malrieu, J. P.; Caballol, R. *J. Chem. Phys.* **2002**, *116*, 2727.

(18) (a) Willett, R. D. In *Magneto-Structural Correlation in exchange coupled systems*; Willett, R. D., Gatteschi, D., Khan, O., Eds.; NATO Advanced Studies Series C, Vol. 140; Reidel: Dordrecht, Netherlands, 1985; pp 389−420. (b) Maass, G.; Gerstein, B.; Willett, R. D. *J. Chem. Phys.* **1967**, *46*, 401. (c) O'Bannon, G.; Willett, R. *Inorg. Chim. Acta* **1983**, *53*, 6131.

(19) Chaudhuri, P.; Oder, K.; Wieghardt, K.; Nuber, B.; Weiss, J. *Inorg. Chem*. **1986**, *25*, 2818.

(20) Figgis, B. N.; Martin, R. L. *J. Chem. Soc*. **1956**, 3837.

(21) Güdel, H. U.; Stebler, A.; Furer, A. *Inorg. Chem*. **1979**, *18*, 1021.

(22) (a) Sulewski, P. E.; Fleury, P. A.; Lyons, K. B.; Cheong, S. W.; Fisk, Z. *Phys. Rev. B* **1990**, *41*, 225. (b) Singh, R. P.; Fleury, P. A.; Lyons, K. B.; Sulewski, P. C. *Phys. Rev. Lett.* **1989**, *62*, 2736.

(23) (a) Aeppli, G.; Hayden, S. M.; Mook, H. A.; Fisk, Z.; Cheong, S. W.; Rytz, D.; Remeika, J. P.; Espinosa, G. P.; Cooper, A. S. *Phys. Rev. Lett*. **1989**, *62*, 2052. (b) Endoh, Y.; Yamada, K.; Birgeneau, R. J.; Gabbe, D. R.; Jenssen, H. P.; Kastner, M. A.; Peters, C. J.; Picone, P. J.; Thurston, T. R.; Tranquada, J. M.; Shirane, G.; Hidaka, Y.; Oda, M.; Enomoto, Y.; Suzuki, M.; Murakami, T. *Phys. Rev. B* **1988**, *37*, 7443. (c) Hayden, S. M.; Aeppli, G.; Osborn, R.; Taylon, A. D.; Perring, T. G.; Cheong, S. W.; Fisk, Z. *Phys. Rev. Lett*. **1991**, *67*, 3622.

(24) Gatteschi, D.; Goslar, J.; Hilczer, W.; Hoffmann, S. K.; Zanchini, C. *Inorg. Chem.* **1996**, *35*, 1148.

(25) Miralles, J.; Castell, O.; Caballol, R.; Malrieu, J. P. *Chem. Phys.* **1993**, *172*, 33.

(26) Cabrero, J.; Ben Amor, N.; de Graaf, C.; Illas, F.; Caballol, R. *J. Phys. Chem. A* **2000**, *104*, 9983.

(27) (a) Calzado, C. J.; Sanz, J. F.; Malrieu, J. P.; Illas, F. *Chem. Phys. Lett*. **1999**, *307*, 102. (b) Calzado, C. J.; Sanz, J. F.; Malrieu, J. P. *J. Chem. Phys*. **2000**, *112*, 5158.

(28) de P. R. Moreira, I.; Illas, F.; Calzado, C. J.; Sanz, J. F.; Malrieu, J. P.; Ben Amor, N.; Maynau, D. *Phys. Rev. B* **1999,** *59*, R6593.

(29) (a) Malrieu, J. P. *J. Chem. Phys.* **1967**, *47*, 4555. (b) Malrieu, J. P.; Claverie, P.; Diner, S. *Theor. Chim. Acta* **1968**, *8*, 404.

(30) Atchity, G. J.; Ruedenberg, K. *J. Chem. Phys.* **1993**, *99*, 3790.

(31) Ruedenberg, K.; Atchity, G. J. *J. Chem. Phys.* **1993**, *99*, 3799.

(32) García, V. M.; Castell, O.; Caballol, R.; Malrieu, J. P. *Chem. Phys. Lett*. **1995**, *238*, 222.

(33) García, V. M.; Reguero, M.; Caballol, R.; Malrieu, J. P. *Chem. Phys. Lett*. **1997**, *281*, 161.

(34) (a) Noodleman, L.; Norman, J. G., Jr. *J. Chem. Phys.* **1979**, *70*, 4903. (b) Noodleman, L. *J. Chem Phys.* **1981**, *74*, 5737. (c) Noodleman, L.; Davidson, E. R. *Chem. Phys.* **1986**, *109*, 131. (d) Noodleman, L.; Peng, C. Y.; Case, D. A.; Mouesca, J. M. *Coord. Chem. Rev.* **1995**, *144*, 199.

(35) Fabrizi de Biani, F.; Ruiz, E.; Cano, J.; Novoa, J. J.; Alvarez, S. *Inorg. Chem*. **2000**, *39*, 3221.

(36) Ruiz, E.; Cano, J.; Alvarez, S.; Alemany, P. *J. Am. Chem. Soc*. **1998**, *120*, 11122.

(37) Frisch, M. J.; Trucks, G. W.; Schlegel, H. B.; Scuseria, G. E.; Robb, M. A.; Cheeseman, J. R.; Zakrzewski, V. G.; Montgomery, J. A., Jr.; Stratmann, R. E.; Burant, J. C.; Dapprich, S.; Millam, J. M.; Daniels, A. D.; Kudin, K. N.; Strain, M. C.; Farkas, O.; Tomasi, J.; Barone, V.; Cossi, M.; Cammi, R.; Mennucci, B.; Pomelli, C.; Adamo, C.; Clifford, S.; Ochterski, J.; Petersson, G. A.; Ayala, P. Y.; Cui, Q.; Morokuma, K.; Malick, D. K.; Rabuck, A. D.; Raghavachari, K.; Foresman, J. B.; Cioslowski, J.; Ortiz, J. V.; Stefanov, B. B.; Liu, G.; Liashenko, A.; Piskorz, P.; Komaromi, I.; Gomperts, R.; Martin, R. L.; Fox, D. J.; Keith, T.; Al-Laham, M. A.; Peng, C. Y.; Nanayakkara, A.; Gonzalez, C.; Challacombe, M.; Gill, P. M. W.; Johnson, B. G.; Chen, W.; Wong, M. W.; Andres, J. L.; Head-Gordon, M.; Replogle, E. S.; Pople, J. A. *Gaussian 98*, revision A.3; Gaussian, Inc.: Pittsburgh, PA, 1998.

(38) Caballol, R.; Sánchez-Marcos, E.; Barthelat, J. C. *J. Phys. Chem.* **1987**, *91*, 1328.

(39) Adamo, C.; Barone, V.; Bencini, A.; Totti, F.; Ciofini, I. *Inorg. Chem*. **1999**, *38*, 1996.

(40) Caballol, R.; Castell, O.; Illas, F.; de P. R. Moreira, I.; Malrieu, J. P. *J. Chem. Phys. A* **1997**, *42*, 7860.

(41) Ovchinnikov, A. A.; Labanowski, J. K. *Phys. Rev*. **1996**, *A53*, 3946.

(42) Calzado, C. J.; Cabrero, J.; Malrieu, J. P.; Caballol, R. *J. Chem. Phys.* **2002**, *116*, 3985.

(43) (a) Bencini, A.; Gatteschi, D.; Zanchini, C. *Inorg. Chem.* **1985**, *24*, 704. (b) Bencini, A.; Gatteschi, D. *J. Am. Chem. Soc.* **1986**, *108*, 5763. (c) Broer, R.; Maaskant, W. J. A. *Chem. Phys.* **1986**, *102*, 103. (d) Miralles, J.; Daudey, J. P.; Caballol, R. *Chem. Phys. Lett.* **1992,** *198*, 555. (e) Castell, O.; Miralles, J.; Caballol, R. *Chem. Phys*. **1994,** *179*, 377.

(44) Andersson, K.; Blomberg, M. R. A.; Fülscher, M. P.; Karlström, G.; Lindh, R.; Malmqvist, P. A.; Neogrády, P.; Olsen, J.; Roos, B. O.; Sadlej, A. J.; Schütz, M.; Seijo, L.; Serrano-Andrés, L.; Siegbahn, P. E. M.; Widmark, P. O. *MOLCAS*, version 4; Lund University: Lund, Sweden, 1997.

(45) CASDI program: Ben Amor, N.; Maynau, D. *Chem. Phys. Lett.* **1998**, *286*, 211.

(46) (a) Caballol, R.; Malrieu, J. P. *Chem. Phys. Lett*. **1992**, *188*, 543. (b) Caballol, R.; Malrieu, J. P.; Daudey, J. P.; Castell, O. *SCIEL program*; Rovira i Virgili University: Tarragona, Spain, 1998.

(47) Schaftenaar, G.; Noordik, J. H. *J. Comput.-Aided Mol. Des.* **2000**, *14*, 123.

(48) (a) Heully, J. L.; Malrieu, J. P. *Chem. Phys. Lett*. **1992**, *199*, 545. (b) Daudey, J. P.; Heully, J. L.; Malrieu, J. P. *J. Chem. Phys*. **1993**, *99*, 1240.

(49) Pitarch-Ruiz, J.; Sánchez-Marín, J.; Maynau, D. *J. Chem. Phys*. **2000**, *112*, 1655.

(50) Becke, A. D. *J. Chem. Phys.* **1993**, *98*, 5648.

(51) Slater, J. C. *Quantum Theory of Molecules and Solids*; McGraw-Hill: New York, 1974; Vol. 4.

(52) Becke, A. D. *Phys. Rev. A* **1988**, *38*, 3098.

(53) Vosko, S. H.; Wilk, L.; Nusair, M. *Can. J. Phys*. **1980**, *58*, 1200.

(54) Lee, C.; Yang, W.; Parr, R. G. *Phys. Rev. B* **1988**, *37*, 785.

(55) (a) Martin, R. L.; Illas, F. *Phys. Rev. Lett*. **1997**, *79*, 1539. (b) Illas, F.; Martin, R. L. *J. Chem. Phys*. **1998**, *108*, 2519.

(56) Calzado, C. J.; Malrieu, J. P. *Chem. Phys. Lett*. **2000**, *317*, 404.

(57) Sodupe, M.; Bertrán, J.; Rodriguez-Santiago, L.; Baerends, E. J. *J. Phys. Chem. A* **1999**, *103*, 166.

(58) (a) Baron, V.; Gillon, B.; Plantevin, O.; Cousson, A.; Mathonière, C.; Kahn, O.; Grand, A.; Öhrström, L.; Delley, B. *J. Am. Chem. Soc.* **1996**, *118*, 11822. (b) Baron, V.; Gillon, B.; Cousson, A.; Mathonière, C.; Kahn, O.; Grand, A.; Öhrström, L.; Delley, B.; Bonnet, M.; Boucherle, J. X. *J. Am. Chem. Soc.* **1997**, *119*, 3500.

(59) Ruiz, E.; Cano, J.; Alvarez, S.; Alemany, P. *J. Am. Chem. Soc*. **1998**, *120*, 11122.

(60) Aebersold, M. A.; Gillon, M.; Plantevin, O.; Pardi, L.; Kahn, O.; Bergerat, P.; von Seggern, I. F. T.; Öhrström, L.; Grand, A.; Lelièvre-Berna, E. *J. Am. Chem. Soc*. **1998**, *120*, 5238.

(61) Cabrero, J.; Bordas, E.; De Graaf, C.; Caballol R.; Malrieu, J. P. *Chem.−Eur. J.*, submitted for publication.